Regulation of secretory granule recruitment and exocytosis at rat neurohypophysial nerve endings

David R. Giovannucci and Edward L. Stuenkel

Department of Physiology, University of Michigan Medical School, Medical Sciences II Building, Ann Arbor, MI 48109, USA

1. Time-resolved cell membrane capacitance (C_m) measurements were used in combination with fura-2 microfluorometry under whole-cell patch clamp recording to investigate the kinetics and Ca^{2+} sensitivity of exocytotic granule fusion evoked by depolarizing stimuli at single, isolated nerve endings of the rat neurohypophysis.

2. Single step depolarizations or trains of depolarizing pulses evoked voltage-dependent, inward Ca^{2+} currents (I_{Ca}) and induced both Ca^{2+}-dependent and Ca^{2+}-independent changes in C_m. Three distinct C_m responses were observed and were differentiated by their kinetics and Ca^{2+} sensitivity: a non-exocytotic transient ($\Delta C_{m,t}$) and an exocytotic C_m 'jump' ($\Delta C_{m,J}$) and a slower, often latent, exocytotic C_m rise ($\Delta C_{m,S}$) that outlasted the depolarizing pulse stimulus.

3. The $\Delta C_{m,t}$ was characterized by a rapid, transient component observed in 70% of nerve endings and a voltage–activation relationship that preceded that of the I_{Ca}. The amplitude and kinetics of the $\Delta C_{m,t}$ were unaffected by I_{Ca} block by Cd^{2+}, Ca^{2+} load reduction, or alterations in intracellular Ca^{2+} buffering.

4. In contrast to the $\Delta C_{m,t}$, both the $\Delta C_{m,J}$ and $\Delta C_{m,S}$ were Ca^{2+} dependent as evidenced by their sensitivity to Cd^{2+} block of I_{Ca}, intraterminal application of 10 mM BAPTA and reduced $[Ca^{2+}]_o$ or replacement of Ca^{2+} as the charge carrier with Ba^{2+}.

5. The $\Delta C_{m,J}$ was proportional to depolarization-evoked Ca^{2+} influx with initial exocytotic rate of approximately 350 granule fusions s^{-1}. The amplitude of the $\Delta C_{m,J}$ rose exponentially ($\tau = 40$ ms) and approached an asymptote (15·5 fF) with longer duration depolarizations indicating the fusion from and depletion of an immediately releasable pool (IRP) estimated at nineteen docked and primed secretory granules.

6. The $\Delta C_{m,S}$ was induced by the application of repetitive long duration pulses and defined as the exocytosis of secretory granules from a readily releasable granule pool (RRP). The $\Delta C_{m,S}$ response occurred only after exceeding a $[Ca^{2+}]_i$ threshold value and rose thereafter in proportion to Ca^{2+} influx with a mean initial secretory rate of 36 granule fusions s^{-1}. The mean latency for $\Delta C_{m,S}$ activation was 850 ms following the initiation of the step depolarizations. The $\Delta C_{m,S}$ response magnitude, reflecting the size of the RRP, was dependent on the resting $[Ca^{2+}]_i$ and the nerve ending size, and was depletable using repetitive depolarizations of long duration.

7. Recruitment into and release from the RRP and IRP were differentially sensitive to changes in intraterminal Ca^{2+} buffering conditions. For example, introduction of 5 mM EGTA was shown to have no effect on the evoked IRP but significantly reduced the RRP. In comparison, diminishment of the endogenous Ca^{2+} buffering capacity of nerve endings by treatment with the mitochondrial Ca^{2+} uniporter blocker Ruthenium Red (10 μM) potentiated the RRP size but had no significant effect on the IRP size.

8. The present study indicates that the Ca^{2+}-dependent recruitment of and release from functionally distinct pools of peptide-containing secretory granules in combination with the $[Ca^{2+}]_i$ regulatory properties of neurohypophysial nerve endings may explain both the depletion of peptide release under prolonged stimulus and the potentiation of peptide release observed to occur during recurrent phasic action potential activity in this system.

The spatial and temporal properties of changes in intracellular calcium concentration ($\Delta[Ca^{2+}]_i$) occurring in response to depolarizing impulse activity not only initiate the exocytotic fusion of secretory vesicles or granules with the plasma membrane, but may shape the secretory response as well (Chow, Klingauf, Heinemann, Zucker & Neher, 1996). Yet, it is not known if the capacity of Ca^{2+} to both trigger and tune the exocytotic response results from the Ca^{2+}-dependent modulation of a common set of proteins, functionally defined by their exposure to discrete Ca^{2+} microenvironments, or via multiple, distinct Ca^{2+}-sensitive pathways. At the synapse, the close association of Ca^{2+} entry sites with fusion-competent vesicles at the active zone is believed to allow for a local, rapid rise in $[Ca^{2+}]_i$ and activation of a low affinity Ca^{2+} sensor leading to the induction of membrane fusion and neurotransmitter release (Zucker & Stockbridge, 1983; Llinás, Sugimori & Silver, 1995). Upon the loss of Ca^{2+} influx the Ca^{2+} gradient rapidly dissipates due to diffusion and rapid buffering, and release stops. Neuroendocrine cells, however, lack a morphological correlate of the active zone and peptide- or catecholamine-containing secretory granules are believed not to co-localize with release sites (Pow & Morris, 1989). In chromaffin cells for example, granules are generally estimated to be positioned at a 10-fold greater distance from the cell membrane release sites, where they would sense at least a 10-fold lower $[Ca^{2+}]_i$ compared with that estimated for synaptic vesicles (Burgoyne & Morgan, 1995). Induction of secretion has therefore been found to require more intense or frequent stimulation or greater Ca^{2+} influx, which results in a slower secretory response which is related to a rise in submembranous $[Ca^{2+}]$ (Chow, Klingauf & Neher, 1994). Thus, the time course of submembranous $[Ca^{2+}]_i$ gradient rise and collapse, the distance between the release-ready vesicles and the Ca^{2+} channels, and the degree of intracellular Ca^{2+} buffering has been postulated to largely determine the exocytotic delay and rate (Chow *et al.* 1996).

Alternatively, Ca^{2+} could shape the secretory response through its interaction with specific isoforms of the various Ca^{2+}-binding protein members that comprise the molecular fusion motor. For example, multiple isoforms of synaptotagmin have been shown to exhibit different Ca^{2+} sensitivities (Chapman, Hanson, An & Jahn, 1995; Li, Davletov & Sudhof, 1995) and may be associated with functionally distinct kinetic components of release (Geppert *et al.* 1994). Additionally, Ca^{2+}-sensitive membrane/protein targeting and recycling processes occurring upstream to and downstream from the exocytotic fusion event may act to shape the secretory response kinetics. For example, a rise in $[Ca^{2+}]_i$ in chromaffin cells has been shown to regulate the recruitment of secretory granules from reserve pools into readily releasable pools or the priming of docked granules, to potentiate the subsequent exocytotic response (Bittner & Holz, 1992; Neher & Zucker, 1993; von Ruden & Neher, 1993). Recruitment and priming are distinguished functionally but may involve the same or different structural components. These pre-fusion pathways are distinct from the exocytotic fusion event as they have been shown to be activated maximally at lower $[Ca^{2+}]_i$ and require Mg-ATP (Bittner & Holz, 1992; Hay & Martin, 1992). These processes may reflect the docking of vesicles at the membrane or partial assembly of the molecular fusion machine (Burgoyne & Morgan, 1995) or focal breakdown and reassembly of the cortical F-actin cytoskeleton (Vitale, Seward & Trifaro, 1995) which may modulate the availability of fusion-competent granules. The rab 3-rabphilin complex, and the secretory proteins nSec1 and α/β- and γ-SNAPs (soluble NSF attachment proteins) have each been implicated to play regulatory roles in vesicle docking and priming (De Camilli & Takei, 1996).

The specific purpose of the present study was to characterize the Ca^{2+} requirements of exocytosis and estimate the maximal secretory rate, the immediately releasable vesicle pool size, and the Ca^{2+} dependence and kinetics of a slower phase of secretion in peptidergic nerve endings. We have investigated these properties of exocytosis using the vasopressin- and oxytocin-secreting nerve endings of rat hypothalamic magnocellular neurons. To address these specific questions, we have used a variant of the whole-cell patch clamp method to monitor with high-temporal resolution minute changes in cell membrane capacitance (ΔC_m) reflecting the addition or removal of membrane during exocytotic vesicle fusion and recycling (Joshi & Fernandez, 1988; Lindau & Neher, 1988). Our studies show that neurohypophysial nerve endings possess at least two functionally distinct secretory granule pools that differ in their size, rate of exocytosis, Ca^{2+} sensitivity, and their perhaps proximity to Ca^{2+} entry site.

METHODS

Preparation of isolated rat neurohypophysial nerve endings

Isolated rat neurohypophysial nerve endings were prepared from male Sprague–Dawley rats (200–300 g) following CO_2 asphyxiation and decapitation. The pituitary was isolated and the anterior and posterior lobes were separated. The pars intermedia was gently removed and isolated nerve endings were dissociated by the dispersion of the neural lobe in 100 μl of a buffer containing (mM): sucrose, 270; EGTA, 1; Hepes, 10; pH adjusted to 7·2 with Tris base. Isolated nerve endings were immediately placed onto a clean glass coverslip that formed the bottom of a superfusion/recording chamber. Following a 5 min settling period, the nerve endings were superfused with a physiological saline solution containing (mM): NaCl, 140; Hepes, 40; $KHCO_3$, 5; $CaCl_2$, 2·2; $MgCl_2$, 1; glucose, 10; pH adjusted to 7·2 with NaOH. Total osmolarity in this and all subsequent solutions was monitored by vapor pressure osmometry (model 5500, Wescor, Inc., Logan, UT, USA) and adjusted to 300–305 mosmol l^{-1}. Experiments were performed on spherical nerve endings with diameters that ranged from 4 to 12 μm.

Electrophysiological recording of Ca^{2+} current (I_{Ca}) and C_m

Whole-cell patch clamp methods were used to evoke and record calcium currents (I_{Ca}) and measure ΔC_m from single nerve endings using an Axopatch 200A amplifier (Axon Instruments, Foster City, CA, USA). Patch pipettes were constructed out of 1·5 mm o.d. capillary glass (Drummond Scientific, Broomall, PA, USA), coated with Sylgard elastomer (Dow Corning, Midland, MI, USA) and fire

polished. The patch pipettes had tip resistances of 3·5–9 MΩ and were filled with a standard pipette solution that contained (mM): *N*-methyl-D-glucamine, 140; Hepes, 40; Mg-ATP, 2; GTP, 0·2; Tris-EGTA, 0·1; fura-2, 0·15; pH adjusted to 7·1 with NaOH. For specific experiments, a number of variations on the standard pipette solution were used. Some of these changes included altering the intracellular Ca^{2+} buffering capacity by increasing the EGTA concentration, the replacement of EGTA with the more rapid Ca^{2+} buffer BAPTA, or the addition of the mitochondrial Ca^{2+}-uptake inhibitor Ruthenium Red. For the recording of I_{Ca}, the superfusion solution was changed from physiological saline to a solution containing (mM): tetraethylammonium chloride, 137; $CaCl_2$, 10; $MgCl_2$, 2; Hepes, 10; glucose, 19; pH adjusted to 7·15 with Tris base. The whole nerve ending capacitance (0·9–3·5 pF) and 65–75% of the series resistance (4–30 MΩ) were compensated to eliminate membrane-charging transients and voltage and temporal errors, respectively. High-resolution membrane capacitance measurements under whole-cell patch clamp recording were used to monitor ΔC_m, which directly reflects secretory activity. The fusion of synaptic vesicles or granules to the plasma membrane during exocytosis results in an increase in the total plasma membrane surface area, providing that the rate of exocytosis is much greater than the rate of endocytosis. Time-resolvable changes in C_m were monitored by using a modified phase-tracking method (Joshi & Fernandez, 1988) with a software-based phase-sensitive detector (Pulse Control 4.5, Richard Bookman, University of Miami, FL, USA). A 19·1 kHz sampling rate (16 samples per sinusoidal period) was used to compute one C_m point every 13·31 ms. Calibration pulses of 100 fF and 500 kΩ were generated at the beginning of each trace by the whole-cell compensation circuit and by dithering of the phase-tracking resistor, respectively.

$[Ca^{2+}]_i$ measurement

For the determination of the spatially averaged intraterminal Ca^{2+} concentration ($[Ca^{2+}]_i$), isolated nerve endings were loaded by dialysis through the recording pipette with a Ca^{2+}-sensitive fluorescent indicator. For these experiments, the cell-impermeant fura-2 pentapotassium salt was included in the intracellular recording solution at a concentration of 150 μM (Molecular Probes, Eugene, OR, USA). $[Ca^{2+}]_i$ was monitored by dual-wavelength microspectrofluorometry (SPEX Industries, Edison, NJ, USA). Individual nerve endings were optically isolated using a 10 μm pinhole stop and then illuminated by epifluorescence through a ×40 oil-immersion objective (numerical aperture, 1·30) with alternating excitation wavelengths of 340 and 380 nm. The spatially averaged fluorescence intensities at an emission wavelength of 510 nm were measured as a dual-wavelength sample point every 500 ms by a photon-counting photomultiplier. Fluorescence intensities were converted to $[Ca^{2+}]_i$ using the ratiometric method. This relationship is described by:

$$[Ca^{2+}]_i = K_{eff}((R - R_{min})/(R_{max} - R)),$$

where R_{min} and R_{max} represent the ratios of emitted light under minimal and saturating $[Ca^{2+}]$ conditions, respectively (Grynkiewicz, Poenie & Tsien, 1985). Values for R_{min}, R_{max} and K_{eff} were determined using an *in vivo* calibration technique, as previously described (Stuenkel, 1994). The constant K_{eff}, which describes the effective dissociation constant of the fura-2 indicator in the intraterminal milieu, was determined experimentally and is not the same as the dissociation constant K_d. The R_{min} value was obtained by the dialysis of nerve endings with a pipette solution comprised of (mM): *N*-methyl-D-glucamine, 130; Hepes, 40; EGTA, 10; fura-2, 0·15; pH adjusted to 7·0 with Tris base. The R_{max} value was obtained with using a pipette solution containing (mM): *N*-methyl-D-glucamine, 140; Hepes, 40; $CaCl_2$, 2; fura-2, 0·15; pH adjusted to pH 7·0 with Tris base. In addition, nerve terminals were dialysed with a solution buffered to contain an intermediate free calcium concentration of 0·34 μM. This solution contained (mM): *N*-methyl-D-glucamine, 125; Hepes, 40; EGTA, 10; $CaCl_2$, 4·6; $MgCl_2$, 2·3; fura-2, 0·15; pH adjusted to 7·0 with Tris. Emitted light intensity measurements for 340 and 380 nm excitation wavelengths were recorded for each of these solutions and used to calculate the calibration constants. The K_{eff} value was calculated by substitution of the intermediate free $[Ca^{2+}]$ solution value, along with the values measured for R_{min} and R_{max}, into the equation above. The R_{min}, R_{max} and K_{eff} values were 0·41, 9·7 and 5·8 μM, respectively.

Statistics

All grouped I_{Ca}, $[Ca^{2+}]_i$, or C_m data (n) are expressed as means ± S.E.M., and significance was determined by Student's t test. Curve fits to the data were accomplished by an iterative, non-linear least-squares fitting algorithm using IGOR PRO software version 2.0 (WaveMetrics, Inc., Lake Oswego, OR, USA).

RESULTS

Temporally resolved measurements of exocytosis in nerve endings

Simultaneous measurements of I_{Ca}, $[Ca^{2+}]_i$ and the associated changes in C_m were performed on isolated nerve endings under whole-cell patch clamp and ionic conditions that isolated I_{Ca}. Step depolarizations to +10 mV from a holding potential of −90 mV were used to activate I_{Ca} and induce a rise in $[Ca^{2+}]_i$ and increase in C_m. As shown in Fig. 1, the depolarization-evoked ΔC_m responses can be composed of multiple kinetic components. In response to a single depolarizing pulse, the ΔC_m was most commonly represented (70% of 58 nerve endings tested) by a rapid transient change in C_m ($\Delta C_{m,t}$) followed by a slower return of C_m to baseline over a period of seconds (Fig. 1*A*), whereas other nerve endings (30%) lacked the transient C_m component (Fig. 1*B*). In 26% of the tested nerve endings an additional kinetic component was observed in response to a single depolarization (Fig. 1*B*). Such responses were characterized by an initial rapid jump in C_m followed after some latency by a larger, slower rise in C_m. This rise began after cessation of the step depolarization-induced Ca^{2+} influx, and returned to resting C_m levels after 1–2 min. We interpret the immediate jump and latent changes in C_m as increases in membrane surface area occurring in response to Ca^{2+} influx-activated exocytosis and the subsequent recovery of C_m to resting levels as endocytosis that follows or exceeds the exocytotic response.

Properties of the transient capacitance signal ($\Delta C_{m,t}$)

Under standard recording conditions a single 5 ms depolarizing pulse was found to evoke only a $\Delta C_{m,t}$ in the nerve endings. Figure 2*A* shows the mean response of nine separate nerve endings to a 5 ms pulse. The $\Delta C_{m,t}$ responses were strikingly similar between different nerve endings and the mean response fitted a double exponential with time constants of 22 and 67 ms. A number of experimental observations indicated that this depolarization-induced

$\Delta C_{m,t}$ was not related to a Ca^{2+}-dependent secretory event. For example, the amplitude of the evoked $\Delta C_{m,t}$ was found not to be affected by the bath addition of 100 μM Cd^{2+}, a blocker of voltage-dependent I_{Ca}, by reducing the external [Ca^{2+}] from 10 to 2·2 mM, or by replacement of Ca^{2+} with Ba^{2+} as the charge carrier. Although there was no effect on the $\Delta C_{m,t}$, the I_{Ca} was dramatically altered by these treatments. For example, Cd^{2+} completely blocked the I_{Ca} ($n = 4$). In addition, the reduction of $[Ca^{2+}]_o$ diminished the peak I_{Ca} by 50% ($n = 4$) and Ba^{2+} enhanced the peak I_{Ca} by 3-fold ($n = 5$). Moreover, inclusion of 10 mM BAPTA in the pipette solution had no significant effect on the kinetics or amplitude of the $\Delta C_{m,t}$ in response to either single or repetitive depolarizations ($n = 7$). Furthermore, a $\Delta C_{m,t}$ was evoked by depolarizing pulses in four nerve endings found to show Na^+ currents but which exhibited neither I_{Ca} nor a sustained C_m increase. Both the $\Delta C_{m,t}$ and the sustained increase in C_m were reduced by 90% ($n = 4$) when Ca^{2+} was omitted from the bath.

The gating kinetics of voltage-dependent channels can produce phase-shifted currents that can project onto a capacitance trace (Debus, Hartmann, Kilic & Lindau, 1995) and a gating charge movement associated with inactivation of Na^+ channels has been correlated with a non-exocytotic C_m transient in rat adrenal chromaffin cells (Horrigan & Bookman, 1994). Therefore, a series of experiments was performed on the nerve endings to determine if the $\Delta C_{m,t}$ was related to voltage-activated charge movement within

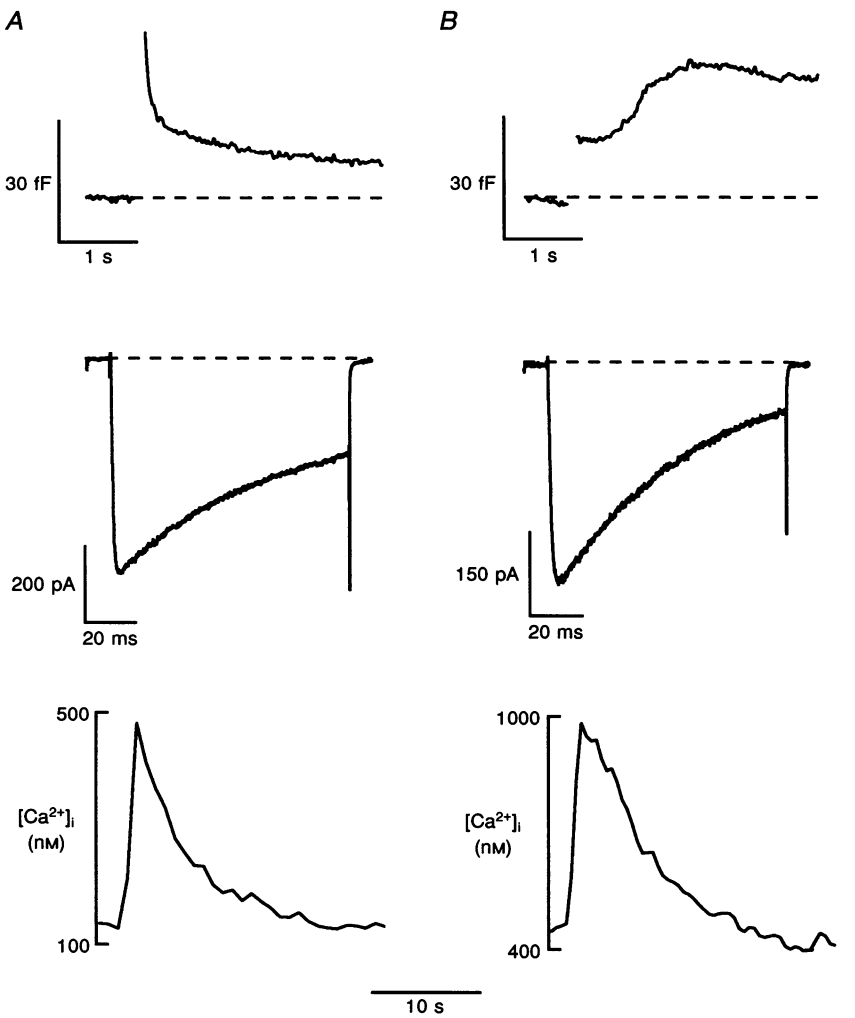

Figure 1. Representative C_m traces from two nerve endings (top panels) and the associated changes in I_{Ca} and $[Ca^{2+}]_i$ (middle and lower panels, respectively) evoked by a single 100 ms depolarization to +10 mV from a holding potential of −90 mV

The portion of the C_m trace corresponding to the duration of the voltage step was omitted because accurate measurement of the ΔC_m during activation of the I_{Ca} is unreliable. *A*, the most common profile showed a rapid, transient change in C_m ($\Delta C_{m,t}$) together with an immediate jump in C_m and followed by a slower return to resting C_m levels. *B*, other nerve endings lacked the $\Delta C_{m,t}$ but exhibited a 'jump' ($\Delta C_{m,J}$) and/or latent C_m rise ($\Delta C_{m,S}$) following cessation of the depolarizing stimulus. Dashed lines indicate baselines for each trace.

the plasma membrane. Figure 2*B* and *C* shows the relationship of the $\Delta C_{m,t}$ amplitude to both the step potential and pulse duration. The amplitude–voltage relationship shows that the $\Delta C_{m,t}$ response was first distinguishable at depolarizations to −40 mV and rose steeply in amplitude over the next 50 mV. A comparison of this profile to the voltage dependence of the I_{Ca} (see Fig. 3*B*) showed that the I_{Ca} inducement lagged $\Delta C_{m,t}$ inducement. Furthermore, whereas the I_{Ca} followed a bell-shaped relationship, the magnitude of the $\Delta C_{m,t}$ rose to a plateau value. Maximal $\Delta C_{m,t}$ activation was observed even when nerve endings were briefly depolarized to a test potential where there was no measurable I_{Ca} (+70 mV). The $\Delta C_{m,t}$ was observed to saturate with pulse durations greater than 50 ms (Fig. 2*C*). Application of rapid, repetitive step depolarizations (10 Hz) failed to exhaust the $\Delta C_{m,t}$ component as might be expected of a pool of immediately releasable granules. The above results strongly suggest that the $\Delta C_{m,t}$ does not represent exo–endocytotic activity and that it is more probably related to a charge redistribution within the membrane.

The presence of the $\Delta C_{m,t}$ together with slower Ca^{2+}-dependent C_m components obfuscates the correct estimation of the initial Ca^{2+}-dependent C_m jump and the initial kinetics of release. Therefore, a correction was performed on ΔC_m responses to isolate the Ca^{2+}-dependent ΔC_m. This was accomplished by performing a point-by-point subtraction of

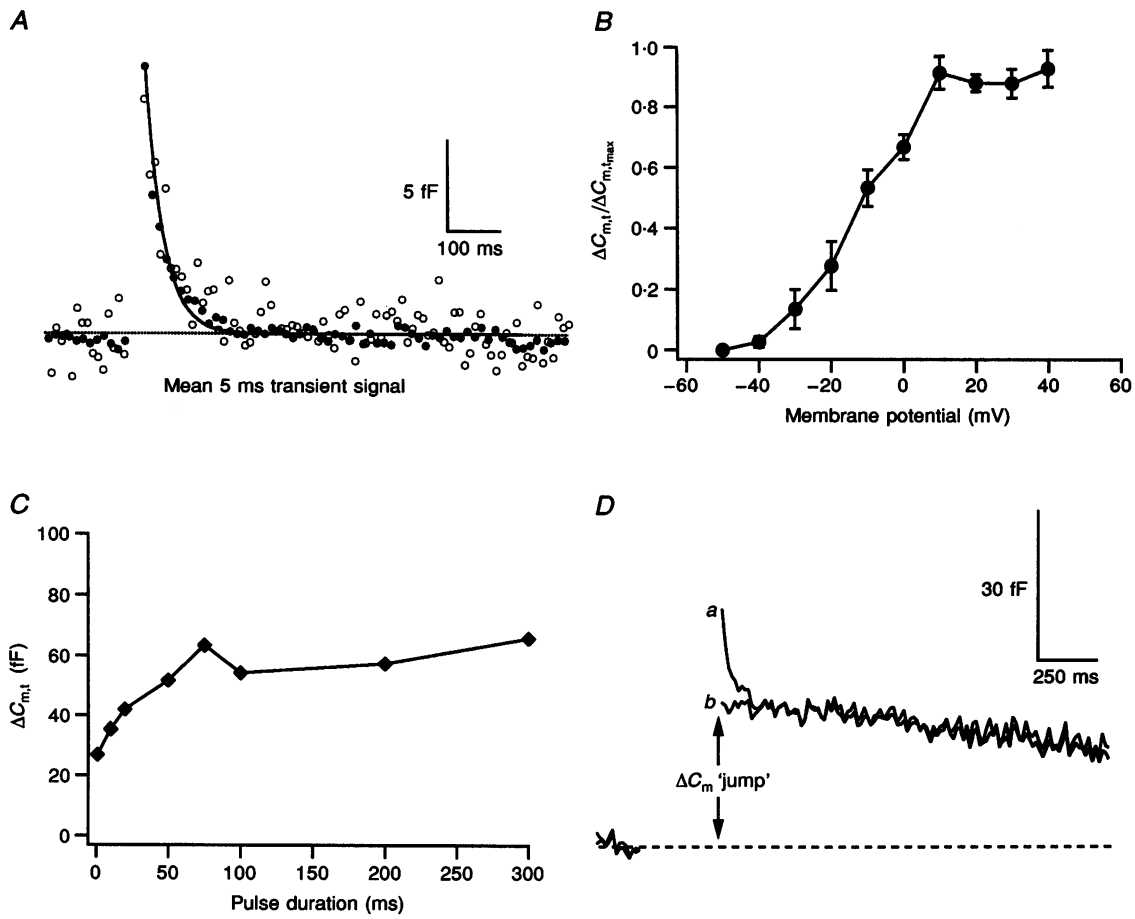

Figure 2. Properties of the non-exocytotic $\Delta C_{m,t}$

A, a 5 ms depolarization evoked only the $\Delta C_{m,t}$. ●, mean ΔC_m trace of nine nerve endings to a 5 ms pulse fitted by a double-exponential curve (continuous line). The $\Delta C_{m,t}$ kinetics are not significantly affected by increased Ca^{2+} buffering as shown by the mean ΔC_m evoked by a 5 ms pulse from nerve endings dialysed with 10 mM BAPTA (○). *B*, to determine the voltage dependency of the $\Delta C_{m,t}$, changes in C_m evoked by a 50 ms pulse from a holding potential of −90 mV were measured on steps to the indicated test potentials. Nerve endings were dialysed with 10 mM BAPTA to isolate the $\Delta C_{m,t}$ from Ca^{2+}-dependent C_m. Each point represents the mean ($7 \geqslant n \geqslant 3$) evoked $\Delta C_{m,t}$ normalized to the maximum $\Delta C_{m,t}$ ($\Delta C_{m,t_{max}}$) amplitude for each nerve ending. *C*, effects of pulse duration on the $\Delta C_{m,t}$ revealed that the $\Delta C_{m,t}$ amplitude rapidly saturates. *D*, isolation of the exocytotic 'jump', $\Delta C_{m,J}$, from the non-exocytotic $\Delta C_{m,t}$ was achieved by alignment and point-by-point subtraction of a 5 ms depolarization-evoked C_m trace determined for each nerve ending. An example of this is shown by the uncorrected (*a*) and corrected (*b*) traces obtained in response to a single 200 ms depolarization.

5 ms ΔC_m data (which elicited only a $\Delta C_{m,t}$) from ΔC_m data obtained from pulses of longer duration (Fig. 2*D*). Generally, a 5 ms pulse was performed for all nerve endings studied. However, in a few experiments 5 ms pulse data were not available and the mean 5 ms $\Delta C_{m,t}$ data (see Fig. 2*A*) were used for subtraction. All data subsequently shown reflect only $\Delta C_{m,t}$-subtracted records.

Properties of the jump in C_m ($\Delta C_{m,J}$)

In contrast to the $\Delta C_{m,t}$, conditions that reduced the I_{Ca} profoundly altered the step depolarization-induced immediate jump in C_m ($\Delta C_{m,J}$). Cd^{2+} (100 μM) was found to abolish both the I_{Ca} and the $\Delta C_{m,J}$ (Fig. 3*A*). Furthermore, the $\Delta C_{m,J}$ responses to depolarizing pulses were abolished when nerve endings were dialysed with pipette solutions containing 10 mM BAPTA. The removal of Ca^{2+} from the bath or a 5-fold reduction in the $[Ca^{2+}]$ abolished or reduced (by 90%) the $\Delta C_{m,J}$ amplitude in response to depolarizing stimuli, respectively ($n = 4$). Compared with Ca^{2+}, Ba^{2+} was shown to be significantly less effective at evoking the $\Delta C_{m,J}$ despite a 3-fold enhancement of the voltage-activated current.

Figure 3*B* illustrates the mean Ca^{2+} current–voltage relationship obtained in response to step depolarizations (75 ms) from a holding membrane potential of −90 mV ($18 \geqslant n \geqslant 4$). Pulses were applied in a randomized series to membrane potentials between −60 and +60 mV, and changes in $[Ca^{2+}]_i$ and C_m were monitored simultaneously and allowed to return to baseline (approximately 30–60 s) before initiating the next pulse in the series. Activation of the inward I_{Ca} began at −30 mV and reached a maximum at +10 mV. The peak I_{Ca} on steps to +10 mV from a holding potential of −90 mV averaged −260 ± 80 pA ($n = 12$). The amplitude of the corresponding increases in membrane capacitance and in intraterminal calcium closely followed the current–voltage profile, and also reached a maximum at +10 mV. The mean increase in $[Ca^{2+}]_i$ in response to a 75 ms step potential to +10 mV was 379 ± 40 nM ($n = 5$) above basal (195 ± 38 nM, $n = 10$). This resting $[Ca^{2+}]_i$ level was consistent with measurements previously reported for this preparation with elevated extracellular Ca^{2+} (Stuenkel, 1994). The above results indicate that the $\Delta C_{m,J}$ represents the Ca^{2+}-dependent fusion of granules from a small, immediately releasable pool, or IRP.

Properties of the slow rise in C_m

Single pulse protocols in certain nerve endings generated a slow component of the ΔC_m, which we term the latent secretory phase ($\Delta C_{m,S}$), that began to rise after the $\Delta C_{m,J}$ and completion of the I_{Ca}. In two nerve endings, the $\Delta C_{m,S}$ was seen with pulse durations as short as 25 ms, although generally, this latent component of the ΔC_m was seen in nerve endings receiving long duration step depolarizations or repetitive depolarizing pulses, or in those exhibiting higher resting $[Ca^{2+}]_i$. Representative responses are shown in Fig. 4*A* and *B*. In nerve endings where a $\Delta C_{m,S}$ was generated by a single depolarizing pulse, the mean peak I_{Ca}, Ca^{2+} influx, resting $[Ca^{2+}]_i$ and $\Delta[Ca^{2+}]_i$ for the shortest duration pulse that elicited the $\Delta C_{m,S}$ were 309 ± 56 pA, 14 ± 4 pC (6·8 ± 1·5 pC pF^{-1}), 333 ± 27 nM and 342 ±

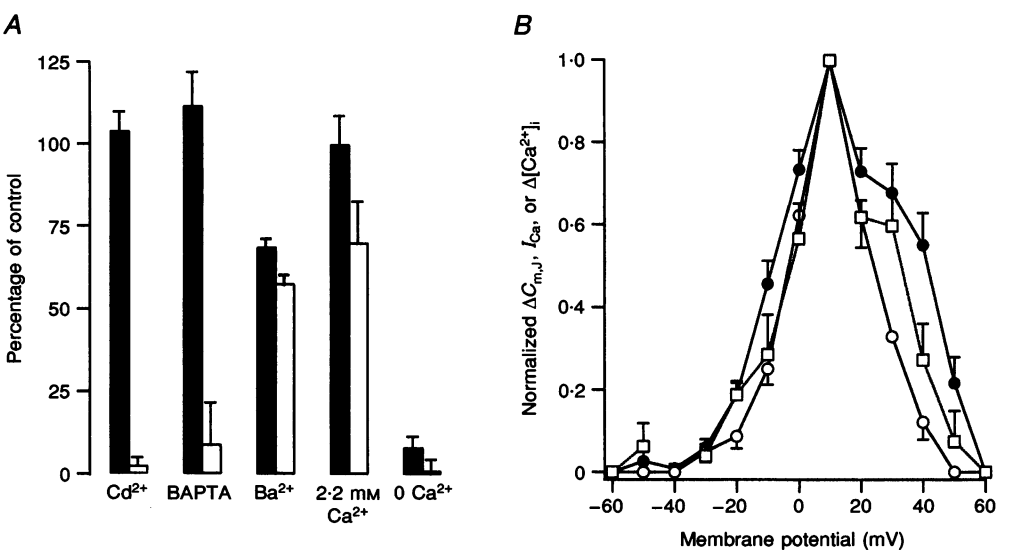

Figure 3. Ca^{2+} dependency of the exocytotic $\Delta C_{m,J}$

A, comparison of the mean $\Delta C_{m,t}$ amplitude (■) and $\Delta C_{m,J}$ (□) obtained under Cd^{2+} block (100 μM) or different Ca^{2+} loads (10 mM BAPTA applied intracellularly via pipette, 10 mM Ba^{2+} substituted extracellularly for Ca^{2+}, or reduced extracellular Ca^{2+} concentration). Measurements were expressed as percentages of the control (10 mM Ca^{2+}). *B*, the voltage relationship of the $\Delta C_{m,J}$ (●) was shown to follow a bell-shaped relationship that correlated with the voltage-dependent activation and inactivation of the I_{Ca} (○) and the $\Delta[Ca^{2+}]_i$ (□). Each point represents the mean $\Delta C_{m,J}$, peak I_{Ca}, or peak $\Delta[Ca^{2+}]_i$, evoked by a 75 ms depolarization from a holding potential of −90 mV ($18 \geqslant n \geqslant 4$) normalized to the maximal response for each nerve ending.

67 nM, respectively ($n = 9$). On average, the $\Delta C_{m,S}$ began to rise 854 ± 71 ms ($n = 11$) after the onset of depolarization and reached a mean maximum ΔC_m of 49 ± 6 fF ($n = 11$). However, the onset of the $\Delta C_{m,S}$ varied considerably between nerve endings.

Applications of trains of eight to ten depolarizing pulses (−90 to +10 mV, 5 Hz) of 50–200 ms duration resulted in one of two types of 'slow' ΔC_m profiles. One type observed in 60% of nerve endings ($n = 25$) consisted of a monophasic response that could be fitted by a single exponential and appeared to lack a latent or persistent component (Fig. 4*C*). In this type of response, successive pulses evoked additional secretory responses that were eventually depleted. However, the magnitude and initial rate of these ΔC_m responses were larger and slower than those determined for the IRP, but closely resembled, in size and rate of rise, a secondary, post-threshold rise in C_m (see below). This second type of C_m response, observed in the remaining 40% of nerve endings tested, was at least biphasic (Figs 4*D* and 5*A*). This inflection in the rising phase of the C_m trace indicated that a significant $\Delta C_{m,S}$ was induced only after a threshold value of Ca^{2+} influx under standard buffering conditions was overcome (Fig. 5*B*). The posterior pituitary contains roughly equal amounts of vasopressinergic and oxytocinergic nerve endings and thus it is tempting to speculate that the qualitative differences in the $\Delta C_{m,S}$ profiles reflect different nerve ending subtypes. However, we feel a more probable explanation is that in some nerve endings the threshold level for RRP (release-ready granule pool) activation is overcome by Ca^{2+} entry with the first depolarizing pulse. Threshold Ca^{2+} values for secretion have been previously reported for this preparation (Lindau, Stuenkel & Nordmann, 1992; Seward, Chernevskaya & Nowycky, 1995). We observed that the initiation of the $\Delta C_{m,S}$ appeared to be related to the cumulative amount of Ca^{2+} influx. This is consistent with a recent report by Seward *et al.* (1995), which proposed that the cumulative number of Ca^{2+} ions that enter during repetitive depolarizations is required to overcome a threshold and activate secretion in neurohypophysial nerve endings. Using C_m measurements in combination with $[Ca^{2+}]_i$ measurements, the present study evaluated whether or not the $\Delta C_{m,S}$ was coupled directly to the number of Ca^{2+} ions entering or to rises in $[Ca^{2+}]_i$. Under our experimental conditions, a mean influx of 25 ± 5·3 pC ($7{\cdot}8 \times 10^7$ Ca^{2+} ions, $n = 8$) was required to evoke the $\Delta C_{m,S}$ response, nearly 4 times the value estimated from Seward *et al.* (1995) to overcome the threshold for secretion (2×10^7 Ca^{2+} ions). Attainment of this threshold may reflect the activation of a Ca^{2+}-dependent priming step for the latent phase secretion by this distal rise in $[Ca^{2+}]_i$. Because our $[Ca^{2+}]_i$ measurements report global changes in intraterminal Ca^{2+}, but lack the spatiotemporal resolution to discern sub-membranous domains of elevated Ca^{2+}, we cannot directly measure this threshold. However, if the activation of the $\Delta C_{m,S}$ depended solely on influx close to the channel pore or a Ca^{2+} μ-domain, then $\Delta C_{m,S}$ should have correlated more with influx than with $[Ca^{2+}]$, as we have shown for the $\Delta C_{m,J}$. The $\Delta C_{m,S}$ was found, however, to require multiple pulses for activation (in many cases) and appeared sensitive to Ca^{2+} diffusion and exogenous buffering. For example, the number of ions entering required to overcome threshold value decreases in proportion with higher resting $[Ca^{2+}]$ and to decreasing terminal size. As shown in Fig. 5*C*, at lower

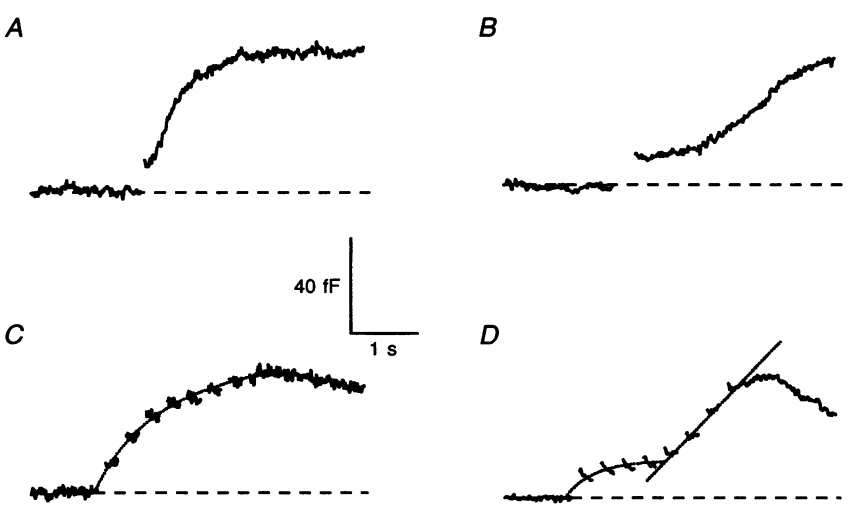

Figure 4. Activation of a slow component of exocytotic secretion ($\Delta C_{m,S}$) by a single or repetitive depolarization protocol

Slow components of the ΔC_m could be evoked by long single step depolarizations (*A* and *B*, 50 ms and 200 ms, respectively) or by the application of repetitive step depolarizations (*C* and *D*, 100 ms at 5 Hz). ΔC_m traces are from four different nerve endings. Note that in *A*, *B* and *D*, the depolarizing stimulus induced both the $\Delta C_{m,J}$ and $\Delta C_{m,S}$ components. Eight to ten 100 ms pulses applied at 5 Hz generally saturated the $\Delta C_{m,S}$ response and were shown to follow a single-exponential curve (*C*) or a more kinetically complex profile (*D*).

resting $[Ca^{2+}]_i$ levels (250–350 nM) a greater number of entering Ca^{2+} ions was required to evoke the $\Delta C_{m,S}$. Conversely, in nerve endings with higher resting $[Ca^{2+}]_i$ levels (350–750 nM) substantially fewer Ca^{2+} ions were required to evoke the $\Delta C_{m,S}$. On average, an absolute rise in the spatially averaged $[Ca^{2+}]_i$ to $\geqslant$ 720 nM was necessary to observe the $\Delta C_{m,S}$, a level consistent with that previously reported to be necessary to evoke secretion in these nerve endings (Lindau *et al.* 1992). Furthermore, we compared the required Ca^{2+} influx to overcome threshold for terminals with similar resting $[Ca^{2+}]_i$ under conditions of altered rates of intraterminal Ca^{2+} buffering. Under standard buffering conditions, a threshold value of $7{\cdot}8 \times 10^7$ Ca^{2+} ions was required to evoke the $\Delta C_{m,S}$. However, when 10 μM Ruthenium Red or 1 mM EGTA (which reduced or enhanced intraterminal Ca^{2+} buffering) was included in the pipette solution, the threshold values were $4{\cdot}8 \times 10^7$ ($n = 4$) and $10{\cdot}8 \times 10^7$ ($n = 2$), respectively. In addition to the effects of intraterminal Ca^{2+} buffering, the threshold value was found to increase with terminal size (Fig. 5*D*). For example, $\Delta C_{m,S}$ initiation was shown to require on average approximately 2-fold more Ca^{2+} entry for nerve endings of larger size.

Once this threshold was overcome, however, the $\Delta C_{m,S}$ during the pulse application was found to rise proportionally with the amount of Ca^{2+} entry. A number of nerve endings, however, exhibited a $\Delta C_{m,S}$ that reached maximum after completion of the pulse protocol. This Ca^{2+} influx-decoupled persistence of secretion has also been observed in chromaffin

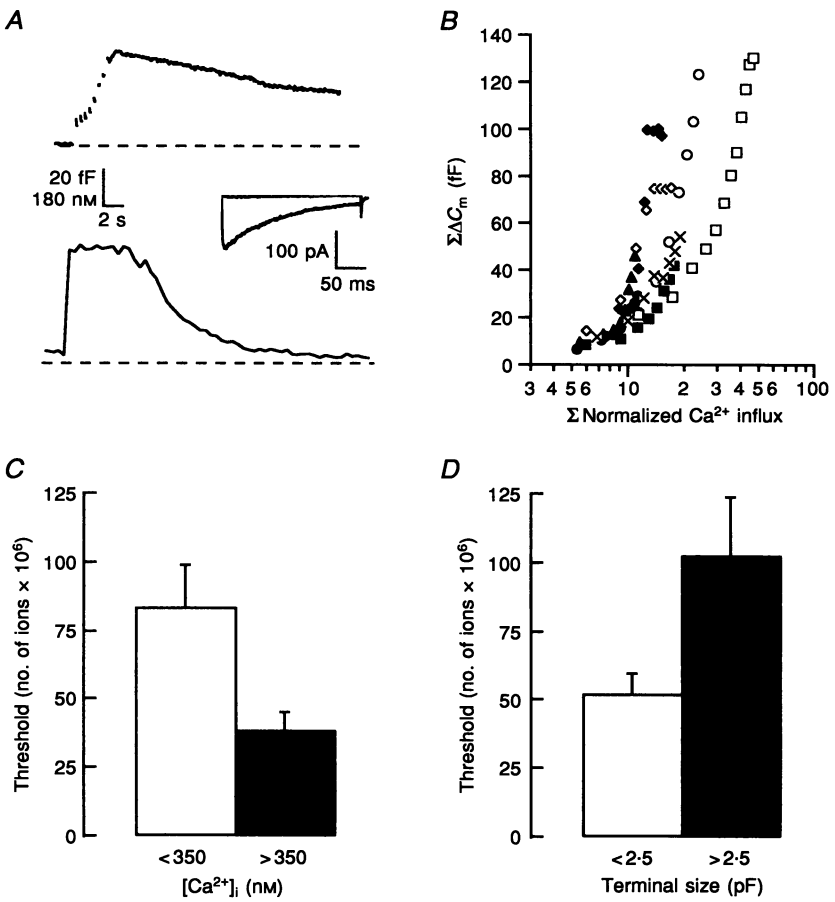

Figure 5. Properties of the latent secretory phase, $\Delta C_{m,S}$

A, representative ΔC_m (top) and corresponding I_{Ca} (middle; first and last evoked currents of the train) and $[Ca^{2+}]_i$ (bottom) traces from a neurohypophysial nerve ending in response to eight 200 ms depolarizations (−90 to +10 mV) at 5 Hz. Note that the inflexion in the rising phase of the ΔC_m trace is interpreted as an activation of the $\Delta C_{m,S}$. *B*, plot of the cumulative ΔC_m *versus* cumulative Ca^{2+} influx evoked by repetitive depolarizations for eight different nerve endings with ΔC_m profiles similar to those shown in *A*. Ca^{2+} influx was normalized to whole terminal membrane capacitance. Above a threshold value, ΔC_m increases proportionally with Ca^{2+} influx. The amount of Ca^{2+} influx required to overcome the threshold value to evoke the $\Delta C_{m,S}$ was related to both nerve ending resting $[Ca^{2+}]_i$ (*C*) and size (*D*). $[Ca^{2+}]_i$ was determined for different nerve endings by fura-2 and placed in bins designated as either low (250–350 nM; $n = 4$) or high $[Ca^{2+}]_i$ (350–750 nM; $n = 4$). Other nerve endings were binned according to size (represented by surface area as determined by whole terminal membrane capacitance) and designated small (1·5–2·5 pF; $n = 4$) or large (2·5–3·5 pF; $n = 5$). Threshold Ca^{2+} values for the induction of the $\Delta C_{m,S}$ were estimated from the inflexion point of the ΔC_m trace.

cells (Augustine & Neher, 1992; Neher & Zucker, 1993; Chow *et al.* 1996; Seward & Nowycky, 1996) and previously in neurohypophysial nerve endings (Lindau *et al.* 1992; Seward *et al.* 1995). Unlike chromaffin cells, however, there seemed to be little direct relationship between Ca^{2+} influx and the maximal $\Delta C_{m,S}$ of neurohypophysial endings. In addition, there was observed to be no strict relationship, higher order or otherwise, between Ca^{2+} influx and the rate of rise of the $\Delta C_{m,S}$ in these nerve endings. Thus, the slow phase of secretion, defined by either the latency of release or by the summation of successive C_m jumps in response to repetitive pulses, probably represents the fusion of granules recruited from a pool that is functionally distinct from that of the IRP.

Determination of the sizes of functionally distinct granule pools

To estimate the size of the IRP and the initial rates of release, we used a series of step depolarizing pulses of increasing duration to deplete the nerve ending of those granules available for immediate release similar to the protocol used in rat adrenal chromaffin cells (Horrigan & Bookman, 1994), goldfish retinal bipolar nerve endings (von Gersdorff & Matthews, 1994), and previously for neurohypophysial slice preparations (Hsu & Jackson, 1996). Figure 6*A* shows the mean $\Delta C_{m,J}$ responses for individual nerve endings ($n = 23$) in response to a random series of depolarizing pulses (−90 to +10 mV) 5–300 ms in duration. The continuous line represents the fitting of the data by a single exponential

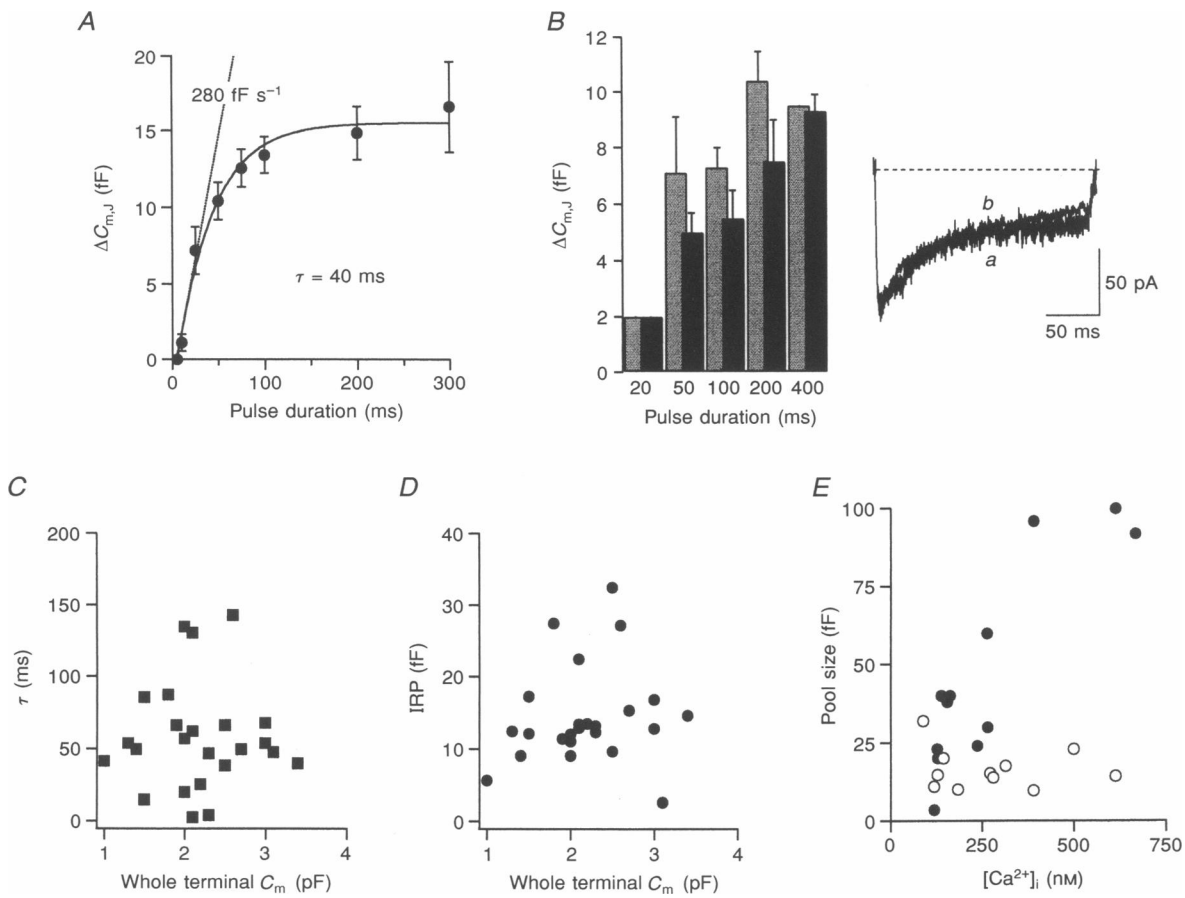

Figure 6. Properties of the immediately releasable granule pool

A, estimation of the immediately releasable secretory granule pool size and the initial rate of secretion. The mean $\Delta C_{m,J}$ evoked by step depolarizing pulses from a holding potential of −90 to 10 mV for different durations applied in a random series to single nerve endings was plotted *versus* pulse duration. The relationship was fitted by a single exponential (continuous line) with a time constant estimated for depletion of 40 ms. The asymptote of this relationship is indicative of the size of the IRP (estimated at 19 granules) and the initial rate of secretion (350 granule fusions s^{-1}) was estimated from a line drawn to the rising phase of the asymptote (dotted line). *B*, a comparison of the $\Delta C_{m,J}$ from six nerve endings evoked by pulses 20–400 ms in duration in either 10 (▨) or 2·2 mM external Ca^{2+} (■). Inset shows the I_{Ca} in response to a 200 ms depolarizing pulse in 2·2 mM Ca^{2+} (*a*) normalized to and superimposed on the I_{Ca} response from the same nerve ending in 10 mM Ca^{2+} (*b*). Data in *A* were pooled from twenty-three nerve endings that ranged in size from 0·9 to 3·5 pF. Neither the time constants of the IRP (*C*) or the size of IRP depletion (*D*) were clearly dependent on nerve ending size. *E*, effects of $[Ca^{2+}]_i$ on the size of the IRP (○) or RRP (●).

with a time constant of 40 ms, which reflects the time course for depletion of the IRP. The mean IRP was estimated from the asymptote of the fit to be 15·5 fF. The mean initial exocytotic rate was estimated at 280 fF s^{-1} and was derived from a linear fit to the rising phase of the asymptote. Assuming a specific C_m of 7·6 fF μm^{-2} (Rosenboom & Lindau, 1994) and a mean secretory granule diameter of 180 nm (Nordmann, 1977), the C_m increases represent an IRP of nineteen granules and an initial exocytotic rate of 350 granule fusions s^{-1}. However, as ΔC_m measurements cannot distinguish between the fusion of granules or microvesicles, or discern concurrent endocytotic activity, these values should represent a lower limit estimate. Notwithstanding, the slower rate of endocytosis compared with that of exocytosis suggests that it would be a greater problem in determining the RRP size than IRP size.

Next, we investigated the possibility that the decreases we have observed in the exocytotic rate might not indicate IRP depletion but instead reflect decreases in the I_{Ca} due to voltage- and Ca^{2+}-dependent Ca^{2+} channel inactivation. We believed this to be unlikely, as the degree of Ca^{2+} influx reduction due to Ca^{2+} channel inactivation ($\tau = 67$ ms) was only one-third of the decrease in the $\Delta C_{m,J}$. We postulated that if the rate of Ca^{2+} channel inactivation were the sole determinant of the saturation of the $\Delta C_{m,J}$ responses occurring to longer duration pulses, then estimates of the IRP achieved under conditions of reduced Ca^{2+} load should be significantly lower than those determined under larger Ca^{2+} loads, assuming that the I_{Ca} inactivation is independent of Ca^{2+} influx. A number of observations regarding the I_{Ca} inactivation properties in these nerve endings indicated that Ca^{2+} channel inactivation in response to a single depolarizing pulse (such as that used to construct the pulse duration–C_m relationship) was not significantly modulated by Ca^{2+} influx. For example, a comparison of eight nerve endings dialysed with either 0·1 mM EGTA or 5 mM EGTA showed no significant difference in the time constant of I_{Ca} inactivation (67 and 62 ms, respectively) of their mean I_{Ca} in response to a 100 ms pulse. No significant slowing of the rate of I_{Ca} inactivation was seen in terminals dialysed with 10 mM BAPTA, or between I_{Ca} recorded under 10 and 2·2 mM external Ca^{2+} concentration (see below). (However, the addition of 10 mM BAPTA abolished the frequency-dependent I_{Ca} inactivation observed in response to repetitive depolarizations (5 Hz) suggesting that Ca^{2+}-dependent Ca^{2+} channel inactivation occurs during repetitive stimulation or that Ca^{2+} may inhibit the recovery from inactivation.) To test if the IRP was in fact an artifact of I_{Ca} inactivation, we used the pulse duration–C_m protocol in the presence of either 10 or 2·2 mM external $[Ca^{2+}]$ in terminals where longer duration single pulses did not evoke the slow component of secretion, and estimated the IRP size. As shown in Fig. 6*B*, in 10 mM Ca_o^{2+}, the $\Delta C_{m,J}$ was found to plateau by 200 ms, whereas 400 ms durations were required to saturate the $\Delta C_{m,J}$ response for the same nerve ending in 2·2 mM Ca_o^{2+}. Consistent with our interpretation that the saturation of the $\Delta C_{m,J}$ response reflects the depletion of an immediately releasable granule pool, we found that the IRP size estimates obtained from fits to the data (such as the relationship shown in Fig. 6*A*) for the same nerve ending under each condition was nearly the same (13 ± 1·4 granules (10 mM) and 12·6 ± 0·8 granules (2·2 mM), $n = 6$). The inset in Fig. 6*B* shows a I_{Ca} obtained under reduced Ca^{2+} load (2·2 mM Ca^{2+}) from a nerve ending in response to a single 200 ms pulse (*a*) and normalized to the response obtained under 10 mM Ca_o^{2+} (*b*) demonstrating that the rates of I_{Ca} inactivation under the two conditions were nearly identical. The time constants of inactivation for the mean I_{Ca} from six nerve endings in 2·2 and 10 mM Ca_o^{2+} were 56 and 45 ms, respectively. In these nerve endings there was found to be no correlation between the rates of I_{Ca} inactivation and the magnitude or time course of $\Delta C_{m,J}$.

In chromaffin cells a correlation between cell size and the size of the IRP has been shown (Horrigan & Bookman, 1994). As shown in Fig. 6*D*, however, no such relationship was discernible for the neurohypophysial nerve endings. IRP pool sizes ranged from 6 to 33 fF ($n = 23$) and had time constants that ranged from 0·9 to 140 ms and which were not related to nerve ending size (Fig. 6*C*).

Release processes in neurohypophysial nerve endings have been shown to fatigue and recover in response to repetitive depolarizing pulse protocols (Fidler Lim, Nowycky & Bookman, 1990). Therefore, it was also possible to obtain an estimate of the mean size of the release-ready granule pool (RRP) from the maximum ΔC_m using repetitive depolarizing pulses to evoke and exhaust a secretory response. Since ΔC_m measurements cannot resolve the origin of granules that fuse, the maximal $\Delta C_{m,S}$ response reflected the sum of contributions of both the IRP and RRP. Therefore, the IRP size was subtracted from the $\Delta C_{m,S}$ maximum to obtain an estimate of the size of the RRP. Generally, the RRP was 2- or 3-fold larger than the IRP. The mean size of the RRP under standard recording conditions (pipette solution containing 0·1 mM EGTA and 0·15 mM fura-2) was estimated at approximately 44 ± 7·3 fF or fifty-five secretory granules ($n = 13$).

Effects of Ca^{2+} buffering capacity on granule pool size

Although neurohypophysial nerve endings showed both immediately and slowly releasable pools of secretory granules, it was not known whether these two pools were governed by the same or different Ca^{2+} requirements. It has been shown in chromaffin cells that an increase in resting $[Ca^{2+}]_i$ prior to release enhances the priming of a release-ready pool of granules (von Ruden & Neher, 1993). We observed a similar effect of resting $[Ca^{2+}]_i$ on the size of the RRP of nerve endings. Figure 6*E* relates the estimated RRP sizes to the resting $[Ca^{2+}]_i$ for twelve different nerve endings. The number of slowly releasable granules increased as resting $[Ca^{2+}]_i$ increased. In contrast, the resting $[Ca^{2+}]_i$ was found to have no corresponding effect on the magnitude of the IRP from the same nerve endings.

A series of experiments were performed to further investigate the relationship between Ca^{2+} and the size of these two kinetically distinct granule pools by controlling $[Ca^{2+}]_i$. The $[Ca^{2+}]_i$ was controlled by setting the Ca^{2+} buffering properties of the patch pipette solution with EGTA or by the addition of Ruthenium Red, which has been previously shown to uncouple a low affinity, high capacity Ca^{2+} buffering mechanism in these nerve endings (Stuenkel, 1994). EGTA at concentrations from 0·1 to 5 mM was found not to block the C_m jump ($\Delta C_{m,J}$). In comparison, as noted above, 10 mM BAPTA completely blocked the Ca^{2+}-dependent $\Delta C_{m,J}$ and $\Delta C_{m,S}$. This difference may result from the slower binding kinetics of EGTA as compared with BAPTA. Figure 7*A* plots the $\Delta[Ca^{2+}]_i$ for nerve endings dialysed with various EGTA concentrations against the Ca^{2+} influx measured as the time-integrated I_{Ca} during the applied step depolarization. To adjust for differences in size or current density, the influx was normalized to the nerve ending size expressed as whole terminal C_m. The relationship of $\Delta[Ca^{2+}]_i$ to Ca^{2+} influx was found to rise exponentially and reach a plateau value with larger Ca^{2+} loads. Increasing the EGTA concentration restored linearity but reduced the

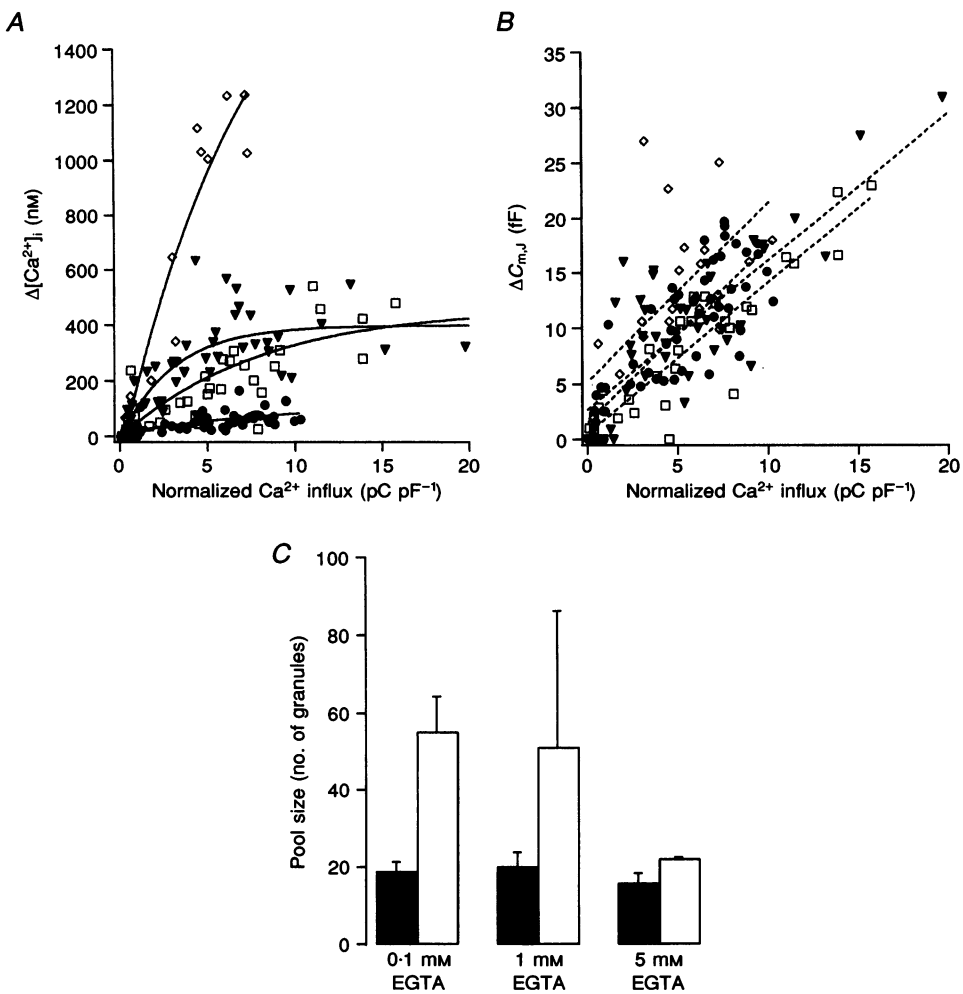

Figure 7. Effects of Ca^{2+} buffering on the evoked $\Delta[Ca^{2+}]_i$ and on secretory granule exocytosis and recruitment

A, relationship of the $\Delta[Ca^{2+}]_i$ to Ca^{2+} influx (time-integrated I_{Ca} evoked by single depolarizations and normalized to whole nerve ending membrane capacitance). Different symbols indicate the different intraterminal buffering conditions achieved by whole nerve ending dialysis with EGTA (0·1–5 mM) or Ruthenium Red (10 μM). Lines represent single-exponential fits of the data points. Parameters (coefficients and estimated errors) of the exponential fitting, respectively: ▼, 0·1 mM EGTA (398 ± 41; −405 ± 67; 0·33 ± 0·13); □, 1 mM EGTA (461 ± 78; −465 ± 75; 0·13 ± 0·04); ●, 5 mM EGTA (127 ± 102; −117 ± 97; 0·09 ± 0·12); ◇, 10 μM Ruthenium Red (2063 ± 1370; −2138 ± 1280; 0·13 ± 0·13). *B*, relationship of the evoked $\Delta C_{m,J}$ to normalized Ca^{2+} influx. Lines represent linear regression fits of the data points. Parameters of the linear fitting, respectively: ▼, 0·1 mM EGTA (2·7 ± 0·98; 1·3 ± 0·13); □, 1 mM EGTA (0·54 ± 0·74; 1·34 ± 0·11); ●, 5 mM EGTA (1·5 ± 0·76; 1·6 ± 0·13); ◇, 10 μM Ruthenium Red (6·7 ± 4; 1·8 ± 0·9). *C*, mean sizes of the immediately (IRP, ■) and readily releasable pools (RRP, □) of secretory granules (see text) for the different intraterminal buffering conditions.

magnitude of the $\Delta[Ca^{2+}]_i$. In contrast, the $\Delta C_{m,J}$ was found to rise linearly with the Ca^{2+} influx and independently of the $\Delta[Ca^{2+}]_i$. Figure 7*B* plots the $\Delta C_{m,J}$ against the Ca^{2+} influx for various intraterminal buffering conditions. Increasing the EGTA concentration did little to alter the $\Delta C_{m,J}$ magnitude or the slope of this relationship. The insensitivity of the $\Delta C_{m,J}$ to Ca^{2+} buffering by EGTA, and the strict relationship between the amplitude of the $\Delta C_{m,J}$ and Ca^{2+} influx but not the $\Delta[Ca^{2+}]_i$ are consistent with the interpretation that the depolarization-evoked $\Delta C_{m,J}$ results from the fusion of granules that are in close proximity to the sites of Ca^{2+} entry, and that their fusion appears to be governed by submembranous rather than global Ca^{2+} gradients. Figure 7*C* compares the mean estimated sizes for the IRP and RRP from nerve endings dialysed with various Ca^{2+} buffer concentrations. Whereas the IRP was not affected, the RRP size was significantly diminished (from 55 to 22·5 ± 0·5 fF; $n = 13$ and 7, respectively) by a 50-fold increase in EGTA concentration.

As shown in Fig. 7*A*, inclusion of 10 μM Ruthenium Red in the pipette solution reduced the rate of endogenous Ca^{2+} buffering and enhanced the mean $[Ca^{2+}]_i$ responses so that the rises in $[Ca^{2+}]_i$ were more closely proportional to Ca^{2+} influx, consistent with a previous report (Stuenkel, 1994). When administered through the recording pipette, Ruthenium Red was found to have no significant effect on the I_{Ca}. For example, the mean peak I_{Ca} elicited by a 50 ms pulse (−90 to 10 mV) for Ruthenium Red-treated and -untreated nerve endings was 310 ± 56 pA ($n = 5$) and 308 ± 44 pA ($n = 11$), respectively. The effects of the reduced rate of Ca^{2+} buffering induced by Ruthenium Red treatment on the $\Delta C_{m,J}$ and $\Delta C_{m,S}$ were investigated. Ruthenium Red alone was not sufficient to cause secretion since dialysis of nerve endings with this compound in the absence of depolarizing stimuli was found to have no effect on the stability of the resting C_m. Likewise, the $\Delta C_{m,J}$ in response to a depolarizing pulse was not significantly affected by the reduced rate of Ca^{2+} buffering. For example, the mean $\Delta C_{m,J}$ in response to a 50 ms depolarizing pulse was 14·2 ± 2·6 fF ($n = 5$) and 10·5 ± 1·2 fF ($n = 23$) for treated and untreated nerve endings, respectively. In contrast, the exocytotic response evoked by repetitive stimuli was enhanced dramatically, indicating an increase in the size of the RRP. For example, as shown in Fig. 8*A*, repetitive depolarizing pulses evoked a much larger $\Delta C_{m,S}$ in the Ruthenium Red-treated nerve endings than in non-treated even though these nerve endings had I_{Ca} and resting $[Ca^{2+}]_i$ of comparable magnitude (~200 pA and 270 nM, respectively). On average, Ruthenium Red-treated nerve endings responded to repetitive depolarizing pulses with a total ΔC_m of 150 fF with an initial, nearly linear rate of rise (11 fF s^{-1}) which outlasted the depolarizing stimuli ($n = 5$). In contrast, the control C_m response reached a plateau of 44 fF at a rate of 29 fF s^{-1} that was best fitted by a single exponential ($n = 13$). Thus, Ruthenium Red-treated nerve endings had a mean RRP size nearly 4 times that estimated for untreated nerve endings (190 *vs.* 55 granules). To

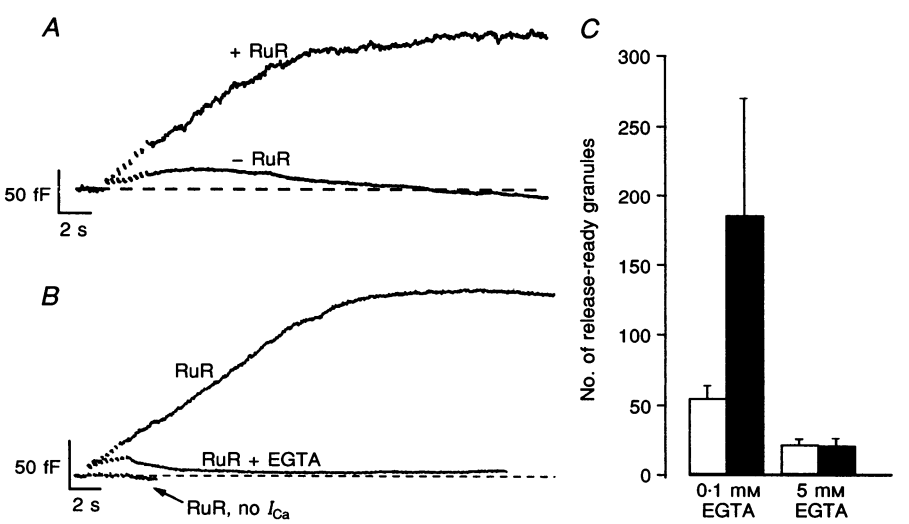

Figure 8. Effects of intraterminal dialysis with Ruthenium Red on the secretory response evoked by repetitive depolarizations

A, a comparison of representative C_m traces demonstrating the enhancement of the evoked ΔC_m response by intracellular dialysis of 10 μM Ruthenium Red (+ RuR) compared with untreated (− RuR) nerve endings. Dashed line indicates baseline membrane capacitance. *B*, a comparison of C_m traces demonstrates the Ca^{2+} dependence of the Ruthenium Red effect. The traces were obtained from Ruthenium Red-treated nerve endings under standard (0·1 mM EGTA) or elevated (5 mM EGTA) buffering conditions, or in a nerve ending which lacked a voltage-activated I_{Ca}. *C*, mean data indicating the size of the readily releasable pool in the presence (■) or absence (□) of Ruthenium Red treatment for low (0·1 EGTA) and high (5 mM EGTA) intraterminal Ca^{2+} buffering conditions.

determine whether or not the $\Delta C_{m,S}$ enhancement was related to the decreased rate of Ca^{2+} buffering or an indirect effect of Ruthenium Red, additional experiments were performed in which 5 mM EGTA was included in the Ruthenium Red-containing pipette solution. Representative C_m traces demonstrating the Ca^{2+} dependency of the Ruthenium Red-enhanced secretion are shown in Fig. 8*B*. The mean $\Delta C_{m,S}$ was limited to $17{\cdot}2 \pm 9$ fF, or 22 ± 11 granules ($n = 5$) when 5 mM EGTA was used to buffer the Ruthenium Red-enhanced changes in $[Ca^{2+}]_i$ (Fig. 8*C*). These data substantiate that, unlike the $\Delta C_{m,J}$, the $\Delta C_{m,S}$ is coupled to the $\Delta[Ca^{2+}]_i$ and not to submembranous Ca^{2+} domains since Ca^{2+} influx was not altered by Ruthenium Red.

DISCUSSION

The present study has examined the regulation of secretory granule recruitment and exocytosis in isolated peptidergic nerve endings of the rat neurohypophysis in response to both single and repetitive depolarizing pulses using whole-cell patch clamp C_m measurements in combination with fura-2 microfluorometric $[Ca^{2+}]_i$ measurements. Exocytotic secretion in nerve endings was shown to occur with at least two functionally distinct Ca^{2+}-sensitive phases, which we have termed the $\Delta C_{m,J}$, characterized by an immediate jump in and rapid recovery of the resting C_m, and the $\Delta C_{m,S}$, typified by a slower C_m rise that persisted after the stimulus. The $\Delta C_{m,J}$ was shown to reflect the exocytotic fusion of a small pool of immediately releasable granules, which proceeded with an initial rate estimated at 280 fF s^{-1}. The magnitude of the $\Delta C_{m,J}$ was related linearly to Ca^{2+} influx and was resistant to pharmacological perturbation of the intrinsic $[Ca^{2+}]_i$ buffering properties of the nerve endings suggesting that this granule pool has close spatial association to the sites of Ca^{2+} entry. In contrast, the $\Delta C_{m,S}$ was less dependent on Ca^{2+} influx than on the absolute $\Delta[Ca^{2+}]_i$ and could be abolished or enhanced by augmenting or inhibiting the rate of $[Ca^{2+}]_i$ buffering with EGTA or with Ruthenium Red treatment. These properties of the $\Delta C_{m,S}$ suggested that it resulted from the fusion of granules from an additional, more slowly released vesicle pool that was at least twice the size of the IRP and which fused with a 10-fold slower rate than that indicated by $\Delta C_{m,J}$.

C_m measurements reveal a non-exocytotic component

The complexity of the ΔC_m response reflects the sensitivity of the C_m monitoring approach which, in addition to exocytotic fusion-dependent responses, can detect changes in C_m that are not related to membrane fusion and surface area changes. For example, the gating kinetics of voltage-dependent channels can produce phase-shifted currents that can project onto a capacitance trace (Debus *et al.* 1995). In chromaffin cells, gating charge movement associated with sodium channel inactivation has been correlated to non-exocytotic C_m transients (Horrigan & Bookman, 1994; Chow *et al.* 1996). We observed a similar $\Delta C_{m,t}$ in the neurohypophysial nerve endings with an amplitude that was independent of Ca^{2+} channel activation and resistant to block by Cd^{2+} or BAPTA. Furthermore, the $\Delta C_{m,t}$ amplitude–membrane potential relationship resulted in an activation curve that resembled a Boltzmann distribution. This would suggest, by similarity to chromaffin cells, that the $\Delta C_{m,t}$ of the nerve endings may also be related to charge redistribution within the membrane occurring during Na^+ channel gating. However, unlike chromaffin cells, the $\Delta C_{m,t}$ of the present study was not found to directly correlate with either the magnitude of Na^+ currents or the kinetics of Na^+ channel inactivation ($\tau = 11$ ms) or recovery from inactivation ($\tau = 7$ ms) (D. Turner, unpublished observations). In addition, the $\Delta C_{m,t}$ of neurohypophysial nerve endings was found to relax approximately an order of magnitude faster (τ, ~60 ms) than the $\Delta C_{m,t}$ attributed to Na^+ channel inactivation in rat chromaffin cells (Horrigan & Bookman, 1994). While the exact cause of the $\Delta C_{m,t}$ in nerve endings remains obscure, it may result from charge movement related to the gating of other voltage-dependent conductances present in these nerve endings. For example, these nerve endings have been shown to contain at least three types of potassium channels (Thorn, Wang & Lemos, 1991; Bielefeldt, Rotter & Jackson, 1992), two of which have kinetics of inactivation fast enough (τ estimated to be between 18–22 and 65–140 ms, respectively) to be considered as possible generators of the $\Delta C_{m,t}$ which exhibits a bi-exponential decay ($\tau = 22$ and 67 ms). Alternatively, phase-tracking can generate a fast transient capacitance response between the pipette and bath solution or between the chamber and microscope. Characteristically, this introduces a phase error and cross-talk between capacitance and conductance traces whose amplitude should be greater at higher access resistances (Gillis, 1995). However, we found no correlation of the occurrence of the $\Delta C_{m,t}$ with series resistance over the range of 4–30 MΩ for the nerve endings studied.

Properties of the immediately releasable exocytotic granule pool

Time-resolved C_m measurements have indicated that goldfish retinal bipolar nerve endings (von Gersdorff & Matthews, 1994), bovine and rat chromaffin cells (Neher & Zucker, 1993; Horrigan & Bookman, 1994) and rat melanotrophs (Parsons, Coorssen, Horstmann & Almers, 1995) possess pools of 'docked' and 'docked and primed' vesicles that are available for release. Estimated initial release rates from the neuroendocrine cells of these studies range between 300 and 1000 granules s^{-1} with IRP sizes that range from as few as seventeen to as many as several hundred granules. In comparison, glutamate-releasing nerve endings have been shown to secrete with an initial rate estimated at 10 000 vesicles s^{-1} from a pool of about 2000 vesicles (Parsons, Lenzi, Almers & Roberts, 1994; von Gersdorff & Matthews, 1994). In the present study, we report that nerve endings prepared from the rat neurohypophysis have a small IRP and exhibit a moderate initial rate of granule exocytosis that match the secretory systems described above. However, a subpopulation of

neurohypophysial nerve endings has been shown to contain small synaptic-like microvesicles (SLMVs). As noted in the results, C_m measurements alone cannot distinguish between the fusion of SLMVs or granules. The difference in vesicle *versus* granule size would have a large impact on our estimates of the IRP and initial rates of exocytosis. Considering a mean SLMV diameter of 44 nm (Theodosis, Dreifuss, Harris & Orci, 1976), approximately 46 aF $(SLMV)^{-1}$, the estimated IRP and rate of fusion approaches that estimated for glutamatergic nerve endings, 337 vesicles and 6000 vesicles s^{-1}, respectively. However, several lines of evidence strongly suggest that the IRP we have observed is not composed of SLMV membrane fusion events. These are: (1) not all nerve endings contain SLMVs, yet an IRP was evident in nearly all tested nerve endings; (2) SLMVs are more abundant in the smaller nerve endings that were not of appropriate size for our patch clamp method; (3) preliminary experiments with the exo–endocytotic marker dye FM1-43 showed no labelling of a rapidly recycling vesicle pool (authors' unpublished observations); and (4) most SLMVs are not localized near the plasma membrane and there is no evidence for an active zone morphology like that of classical synapses or the neuromuscular junction which facilitates very rapid exocytosis.

The Ca^{2+}-dependent increases in the $\Delta C_{m,J}$ eventually reached a maximum response and we have interpreted this, as have others, as the release from and eventual depletion of an IRP. In addition, we found relatively tight coupling between the I_{Ca} and the $\Delta C_{m,J}$ magnitude in nerve endings, which differed from a less stringent coupling between I_{Ca} and release from the IRP of chromaffin cells (Horrigan & Bookman, 1994). Our observations of an IRP, however, contradict a previous report which concluded that the IRP is absent in isolated neurohypophysial nerve endings (Seward *et al.* 1995). Large C_m jumps in response to single depolarizations were observed in the previous study, but were interpreted as activation of a slow 'secretory phase' occurring in response to Ca^{2+} influx that exceeded a threshold level during the depolarization. The reason for the discrepancy between the reports is unknown. One possibility is that specific differences in the pipette recording solutions or nerve ending preparations account for the observed differences. For example, the dialysis solution $[Cl^-]$ was more than 10-fold higher in the present than in the previous study. Chloride has been shown to enhance the Ca^{2+} sensitivity of exocytosis in rat melanotrophs (Rupnik & Zorec, 1992). The Ca^{2+}-dependent C_m changes reported in the prior study, therefore, probably represent release from the slowly releasable vesicle pool represented by the RRP of the present study. In contrast, a recent study by Hsu & Jackson (1996) using C_m measurements of Ca^{2+}-induced exocytosis in slices prepared from the rat neural lobe is consistent with the present study's demonstration of an IRP and RRP. They also observed a small, rapid component of exocytosis evoked by short duration pulses and a larger slower component revealed by longer pulses which they attribute to two kinetically distinct vesicle pools.

Properties of the slowly released granule pool

Docked and primed granules have been shown to comprise only a portion of the releasable granule pool and an additional, distinct secretory component, or readily releasable pool (RRP) has been reported for both bovine and rat chromaffin cells (Neher & Zucker, 1993; von Ruden & Neher, 1993; Horrigan & Bookman, 1994; Seward & Nowycky, 1996). Rat neurohypophysial nerve endings also appear to possess this component of exocytosis as evidenced by its initiation after a latency and persistence after cessation of the depolarizing stimulus and Ca^{2+} influx (Augustine & Neher, 1992; Chow *et al.* 1996), and we have termed this component the $\Delta C_{m,S}$. The $\Delta C_{m,S}$ resembles the 'secretory phase' or 'slow phase' previously described for neurohypophysial nerve endings and secretion from the RRP of chromaffin cells in kinetics, Ca^{2+} requirement, and modulation by $[Ca^{2+}]_i$ buffering (Lindau *et al.* 1992; Rosenboom & Lindau, 1994; Seward *et al.* 1995).

Under standard experimental conditions, the RRP of neurohypophysial nerve endings was estimated to be approximately 45 fF or fifty-five granules in size. However, whereas estimation of the size of the IRP and initial kinetics of exocytosis by isolating the $\Delta C_{m,J}$ from the $\Delta C_{m,S}$ was relatively straightforward, estimates of the RRP inferred from $\Delta C_{m,S}$ measurements were more difficult since (1) the $\Delta C_{m,J}$ and $\Delta C_{m,S}$ probably overlap, and (2) the plateau of the response in many nerve endings may have been influenced by the inactivation-dependent decrease in I_{Ca}. The former problem was overcome by subtracting the magnitude of the IRP (which could be determined independently from the slow secretory component) from that of the $\Delta C_{m,S}$ determined for a given nerve ending since the amplitude of the $\Delta C_{m,J}$ was found not to be affected by elevated $[Ca^{2+}]_i$. Although increasing pulse duration or interpulse interval had no effect on potentiating the maximal evoked $\Delta C_{m,S}$ response, it is possible that the RRP may not be completely depletable, perhaps due to the fast kinetics of RRP refilling. Thus, our estimates of the RRP must be considered to be a lower limit value.

$[Ca^{2+}]_i$ and Ca^{2+} buffering effects on secretory granule pools

The dynamics of membrane fusion, recycling, and Ca^{2+} channel regulation have been shown to differ between fast neurotransmitter-containing clear synaptic vesicles and peptide-containing dense core granules (Burgoyne & Morgan, 1995). For example, Peng & Zucker (1993) have shown that peptide release from luteinizing hormone-releasing hormone-containing secretory granules of the bullfrog sympathetic ganglia is linearly related to the time integral of the presynaptic Ca^{2+} elevation after exceeding an $[Ca^{2+}]_i$ threshold level, which is strikingly different from the fourth- or fifth-order dependence on Ca^{2+} that characterizes

the release from synaptic vesicles at the neuromuscular junction or synapse. In addition, submembranous $[Ca^{2+}]_i$ domains may be more effective at synaptic vesicle release whereas global rises in $[Ca^{2+}]_i$ may be be more effective at evoking secretory granule release. This may, in part, apply to the docked and fully primed (represented by the IRP) and the docked and readily releasable (RRP) phases of secretion of neurohypophysial nerve endings, where we have found that manipulation of intraterminal Ca^{2+} buffering capacity can differentially modulate release from the IRP or RRP. For example, increased Ca^{2+} chelator concentration profoundly reduced or blocked the $[Ca^{2+}]_i$ and $\Delta C_{m,S}$ but had no effect on the I_{Ca} or $\Delta C_{m,J}$. Furthermore, the Ruthenium Red-induced decreased rate of Ca^{2+} buffering greatly potentiated both the $[Ca^{2+}]_i$ and $\Delta C_{m,S}$ but had no effect on the I_{Ca} or $\Delta C_{m,J}$. By comparison, BAPTA, which is more effective than EGTA at collapsing local Ca^{2+} gradients, abolished the $\Delta C_{m,J}$.

In the present study, we observed that the amount of Ca^{2+} necessary to initiate secretion from the RRP varied proportionally with the size and the resting $[Ca^{2+}]_i$ levels of nerve endings, such that larger nerve endings or those with lower resting $[Ca^{2+}]_i$ levels required greater Ca^{2+} entry to overcome a $[Ca^{2+}]_i$ threshold determined by fura-2 loading to be approximately 700 nM. This would seem to conflict with recent work by Rosenboom & Lindau (1994). Using internal dialysis with high $[Ca^{2+}]$, these researchers evoked maximal secretion (32 fF s^{-1}) in neurohypophysial nerve endings with 50 μM Ca^{2+}. (Note that this rate is similar to our measurements for release from the RRP and not the IRP.) However, it is possible that the 700 nM threshold value represents the generation of a local domain or 'shell' of higher concentration that is necessary to set into motion the process of RRP secretion. In this case, the $[Ca^{2+}]_i$ necessary to drive RRP secretion may be 70-fold greater than that discernible by spatially averaged $[Ca^{2+}]_i$ measurements. As indicated above, however, the sensitivity of the RRP to submembranous $[Ca^{2+}]_i$ was less stringent than that of the IRP and depended on the degree of intraterminal Ca^{2+} buffering. This may reflect the requirement for additional Ca^{2+}-sensitive priming steps or an increased distance between the sites of Ca^{2+} entry and RRP secretory granule release than for the IRP (e.g. the RRP and Ca^{2+} channels are not co-localized). Either of these interpretations is consistent with the correlation of RRP-based secretion to the rise in $[Ca^{2+}]_i$ and the sensitivity of RRP-based secretion to EGTA buffering. Alternatively, the observation that a threshold Ca^{2+} entry level must be overcome to initiate RRP secretion could be explained as the amount of Ca^{2+} necessary to saturate the the exogenous chelator. After such saturation, the spatially averaged Ca^{2+} concentration rises and initiates the exocytosis of granules located some distance away from the Ca^{2+} channels. For example, a nerve ending with a 9 μm diameter and volume of 0·38 pl dialysed with an internal medium concentration of 0·25 mM Ca^{2+} chelator would contain about 6×10^7 Ca^{2+}-binding molecules. This amount would define the maximum binding capacity since both the EGTA and fura-2 used bind Ca^{2+} with 1 : 1 stoichiometry. However, we feel that saturation of the chelator is not the sole predictor of threshold. For example, EGTA is a relatively slow chelator and would probably be overcome by Ca^{2+} entry during the activation of currents of large amplitude. Furthermore, there exists in these nerve endings a large capacity, low affinity Ca^{2+} homeostasis mechanism (probably mitochondrial Ca^{2+} uptake), which limits changes in the spatially averaged Ca^{2+} concentration to 400–500 nM (Stuenkel, 1994), and this, presumably, would render chelator saturation unlikely. However, the most convincing evidence that Ca^{2+} buffer saturation is not the activator of RRP release is that the $[Ca^{2+}]_i$ did not rise concurrently with activation of the $C_{m,S}$. Thus, both the latency and apparent decoupled nature of the rise of the $C_{m,S}$ may indicate the time required for both diffusion of Ca^{2+} from the Ca^{2+} channels to the RRP release sites and for the activation of unknown Ca^{2+}-dependent steps necessary to prepare these granules for secretion.

Physiological significance of functionally distinct components of exocytosis on arginine vasopressin secretion

Only a small percentage of the total peptide store in the posterior pituitary is acutely released and the rate of release evoked by continuous stimulation has been shown to decline with time suggesting that there exists a readily releasable granule pool distinct from the bulk of less readily available granules in the nerve ending (Morris, Chapman & Sokol, 1987). The present study has shown that neurohypophysial nerve endings possess at least two functionally distinct, acutely releasable secretory granule pools that differ in size, rate and Ca^{2+} sensitivity of exocytosis, and perhaps proximity to the Ca^{2+} entry sites or in the degree to which they have been primed for release. We propose that the presence of discrete granule pools, as well as the ability of $[Ca^{2+}]_i$ to adjust the gain of arginine vasopressin release by modulating the number of fusion-competent secretory granules that can be mobilized from the RRP, allows for the 'tuning' of the exocytotic secretory response to a broad range of stimulus demands. The strict coupling between Ca^{2+} influx and release of the IRP-mobilized granules assures a synchronous, measured response of one to a few granule fusions per nerve ending or swelling under conditions of low stimulus demand. Such release would be achieved without raising the $[Ca^{2+}]_i$ to high levels. On the other hand, an increase in the firing rate of patterned bursts of stimuli has been shown to enhance the amount of peptide release per action potential spike (Bourque, 1990). Under conditions of intense, physiological demand for neurohormone release, such as dehydration or haemorrhagic shock, vasopressinergic magnocellular neurons undergo patterned action potential bursting (Poulain & Wakerley, 1982). The ensuing elevation in $[Ca^{2+}]_i$ would mobilize

secretory granules for fusion from the larger, asynchronously released RRP. In addition, the ability of Ca^{2+} to increase the number of docked granules or to prime the depletable RRP could presumably tailor release (gain) as a spike or bolus of arginine vasopressin, even in the presence of continued stimulation.

AUGUSTINE, G. J. & NEHER, E. (1992). Calcium requirements for secretion in bovine chromaffin cells. *Journal of Physiology* **450**, 247–271.

BIELEFELDT, K., ROTTER, J. L. & JACKSON, M. B. (1992). Three potassium channels in rat posterior pituitary nerve terminals. *Journal of Physiology* **458**, 41–67.

BITTNER, M. A. & HOLZ, R. W. (1992). Kinetic analysis of secretion from permeablized adrenal chromaffin cells reveals distinct components. *Journal of Biological Chemistry* **267**, 16219–16225.

BOURQUE, C. W. (1990). Intraterminal recordings from the rat neurohypophysis *in vitro*. *Journal of Physiology* **421**, 247–262.

BURGOYNE, R. D. & MORGAN, A. (1995). Ca^{2+} and secretory-vesicle dynamics. *Trends in Neurosciences* **18**, 191–196.

CHAPMAN, E. R., HANSON, P. I., AN, S. & JAHN, R. (1995). Ca^{2+} regulates the interaction between synaptotagmin and syntaxin 1. *Journal of Biological Chemistry* **270**, 23667–23671.

CHOW, R. H., KLINGAUF, J., HEINEMANN, C., ZUCKER, R. S. & NEHER, E. (1996). Mechanisms determining the time course of secretion in neuroendocrine cells. *Neuron* **16**, 369–376.

CHOW, R. H., KLINGAUF, J. & NEHER, E. (1994). Time course of Ca^{2+} concentration triggering exocytosis in neuroendocrine cells. *Proceedings of the National Academy of Sciences of the USA* **91**, 12765–12769.

DEBUS, K., HARTMANN, J., KILIC, G. & LINDAU, M. (1995). Influence of conductance changes on patch clamp capacitance measurements using a lock-in amplifier and limitations of the phase tracking technique. *Biophysical Journal* **69**, 2808–2822.

DE CAMILLI, P. & TAKEI, K. (1996). Molecular mechanisms in synaptic vesicle endocytosis and recycling. *Neuron* **16**, 481–486.

GEPPERT, M., GODA, Y., HAMMER, R. E., LI, C., ROSAHL, T. W., STEVENS, C. F. & SUDHOF, T. C. (1994). Synaptotagmin 1: a major Ca^{2+} sensor for transmitter release at a central synapse. *Cell* **79**, 717–727.

GILLIS, K. D. (1995). Techniques for membrane capacitance measurements. In *Single-Channel Recording*, ed. SAKMANN, B. & NEHER, E., pp. 155–198. Plenum Press, New York.

GRYNKIEWICZ, G., POENIE, M. & TSIEN, R. Y. (1985). A new generation of Ca indicators with greatly improved fluorescent properties. *Journal of Biological Chemistry* **260**, 3440–3450.

FIDLER LIM, N., NOWYCKY, M. C. & BOOKMAN, R. J. (1990). Direct measurement of exocytosis and calcium currents in single vertebrate nerve terminals. *Nature* **344**, 449–451.

HAY, J. C. & MARTIN, T. F. J. (1992). Resolution of regulated secretion into sequential MgATP-dependent and calcium-dependent stages mediated by distinct cytosolic proteins. *Journal of Cell Biology* **119**, 139–151.

HORRIGAN, F. T. & BOOKMAN, R. J. (1994). Releasable pools and the kinetics of exocytosis in adrenal chromaffin cells. *Neuron* **13**, 1119–1129.

HSU, S.-F. & JACKSON, M. B. (1996). Rapid exocytosis and endocytosis in nerve terminals of the rat posterior pituitary. *Journal of Physiology* **494**, 539–553.

JOSHI, C. & FERNANDEZ, J. M. (1988). Capacitance measurements. An analysis of the phase detector technique used to study exocytosis and endocytosis. *Biophysical Journal* **53**, 885–892.

LI, C., DAVLETOV, B. A. & SUDHOF, T. C. (1995). Distinct Ca^{2+} and Sr^{2+} binding properties of synaptotagmins. *Journal of Biological Chemistry* **270**, 24898–24902.

LINDAU, M. & NEHER, E. (1988). Patch-clamp techniques for time-resolved capacitance measurements in single cells. *Pflügers Archiv* **411**, 137–146.

LINDAU, M., STUENKEL, E. L. & NORDMANN, J. J. (1992). Depolarization, intracellular calcium and exocytosis in single vertebrate nerve endings. *Biophysical Journal* **61**, 19–30.

LLINÁS, R., SUGIMORI, M. & SILVER, R. B. (1995). The concept of calcium concentration microdomains in synaptic transmission. *Neuropharmacology* **34**, 1443–1451.

MORRIS, J. F., CHAPMAN, D. B. & SOKOL, H. W. (1987). Anatomy and function of the classic vasopressin-secreting hypothalamus-neurohypophysial system. In *Vasopressin, Principles and Properties*, ed. GASH, D. M. & BOER, G. J., pp. 1–87. Plenum Press, New York.

NEHER, E. & ZUCKER, R. S. (1993). Multiple calcium dependent processes related to secretion in bovine chromaffin cells. *Neuron* **10**, 21–30.

NORDMANN, J. J. (1977). Ultrastructural morphometry of the rat neurohypophysis. *Journal of Anatomy* **123**, 213–218.

PARSONS, T. D., COORSSEN, J. R., HORSTMANN, H. & ALMERS, W. (1995). Docked granules, the exocytotic burst, and the need for ATP hydrolysis in endocrine cells. *Neuron* **15**, 1085–1096.

PARSONS, T. D., LENZI, D., ALMERS, W. & ROBERTS, W. M. (1994). Calcium-triggered exocytosis and endocytosis in an isolated presynaptic cell: capacitance measurements in saccular hair cells. *Neuron* **13**, 875–883.

PENG, Y. Y. & ZUCKER, R. S. (1993). Release of LHRH is linearly related to the time integral of presynaptic Ca^{2+} elevation above a threshold level in bullfrog sympathetic ganglia. *Neuron* **10**, 465–473.

POULAIN, D. A. & WAKERLEY, J. B. (1982). Electrophysiology of hypothalamic magnocellular neurones secreting oxytocin and vasopressin. *Neuroscience* **7**, 773–808.

POW, D. V. & MORRIS, J. F. (1989). Dendrites of hypothalamic magnocellular neurons release neurohypophysial peptides by exocytosis. *Neuroscience* **32**, 435–439.

ROSENBOOM, H. & LINDAU, M. (1994). Exo-endocytosis and closing of the fission pore during endocytosis in single pituitary nerve terminals internally perfused with high calcium concentrations. *Proceedings of the National Academy of Sciences of the USA* **91**, 5267–5271.

RUPNIK, M. & ZOREC, R. (1992). Cytosolic chloride ions stimulate Ca^{2+}-induced exocytosis in melanotrophs. *FEBS Letters* **303**, 221–223.

RYAN, T. A. & SMITH, S. J. (1995). Vesicle pool mobilization during action potential firing at hippocampal synapses. *Neuron* **14**, 983–989.

SEWARD, E. P., CHERNEVSKAYA, N. I. & NOWYCKY, M. C. (1995). Exocytosis in peptidergic nerve terminals exhibits two calcium-sensitive phases during pulsatile calcium entry. *Journal of Neuroscience* **15**, 3390–3399.

SEWARD, E. P. & NOWYCKY, M. C. (1996). Kinetics of stimulus-coupled secretion in dialyzed bovine chromaffin cells in response to trains of depolarizing pulses. *Journal of Neuroscience* **16**, 553–562.

STUENKEL, E. L. (1994). Regulation of intracellular calcium and calcium buffering properties of rat isolated neurohypophysial nerve endings. *Journal of Physiology* **481**, 251–271.

THEODOSIS, D. T., DREIFUSS, J. J., HARRIS, M. C. & ORCI, L. (1976). Secretion-related uptake of horseradish peroxidase in neurohypophysial axons. *Journal of Cell Biology* **70**, 294–303.

THORN, P. J., WANG, X. M. & LEMOS, J. R. (1991). A fast, transient K^+ current in neurohypophysial nerve terminals of the rat. *Journal of Physiology* **432**, 313–326.

VITALE, M. L., SEWARD, E. P. & TRIFARO, J. M. (1995). Chromaffin cell cortical actin network dynamics control the size of the release-ready vesicle pool and the initial rate of exocytosis. *Neuron* **14**, 353–363.

VON GERSDORFF, H. & MATTHEWS, G. (1994). Dynamics of synaptic vesicle fusion and membrane retrieval in synaptic terminals. *Nature* **367**, 735–739.

VON RUDEN, L. & NEHER, E. (1993). A Ca-dependent early step in the release of catecholamines from adrenal chromaffin cells. *Science* **262**, 1061–1064.

ZUCKER, R. S. & STOCKBRIDGE, N. (1983). Presynaptic calcium diffusion and the time courses of transmitter release and synaptic facilitation at the squid giant synapse. *Journal of Neuroscience* **3**, 1263–1269.

Acknowledgements

This work was supported by National Institutes of Health (NS31888) and National Science Foundation (IBN-9410834) grants to E. L. Stuenkel and an American Heart Association/Michigan Affiliate Postdoctoral Fellowship (09F956) to D. R. Giovannucci.

Author's email address

D. R. Giovanucci: luddite@umich.edu

Received 10 June 1996; accepted 22 October 1996.